CHAPTER 6
THE EFFECTS OF Al-CONTAINING WASTE FINENESS ON PROPERTIES OF AUTOCLAVE AERATED CONCRETE INCORPORATING RHA

6.1 Introduction

Although, the incorporation of RHA in AAC reduced both the dry density and compressive strength, the sand replacement ratio by RHA of 75% and 100% by weight met the standard requirements of AAC-6 and AAC-4, respectively, following ASTM C1386 [60]. In regards to the microstructure, the high concentration of RHA (75% and 100%) presented tobermorite crystalline at temperatures of 180°C over 2 hr, whereas the other ratios showed CSH. This means that the utilization of RHA in AAC could reduce energy consumption through the reduction of autoclaving times and temperatures. This has opened the door for combining other industrial waste by-products in AAC.

The other waste used in this study was non-metallic residue (NMP), which normally is sent out from the aluminium dross recovery process. Typically, NMP contains high concentrations of aluminium oxide (Al_2O_3) and up to 5% of metallic aluminium, which could act as a pore-forming agent in AAC production. Therefore, this work looks at the possibility of using solid residue from the aluminium dross recovery process (AW) and rice husk ash (RHA) for producing AAC. RHA was used as a partial substitution for fine aggregate, whereas AW was used as a partial pore-forming agent for AAC. Moreover, it is well know that an increase in the fineness of materials could enhance the reactivity. Therefore, the effect of AW fineness on physical, mechanical and microstructural properties of AAC incorporating RHA was also investigated.

6.2 Materials

The rice husk ash (RHA) used in this study was synthesized by firing in an electric furnace at a temperature of 650 °C for 1 h and then was ground to be retained on sieve No. 325 under 34% by weight, in accordance with ASTM C618 [48]. The silica present in RHA was examined by X-ray diffraction (XRD; Miniflex using Cu Kα radiation (1λ = 1.5406 Å) at a voltage of 40 kV and 40 mA). A broad peak characteristic of amorphous SiO_2 was present at 2θ of around 23 degrees. Quartz sand was also ground to an average

particle size of approximately 100 μm. Aluminium powder was provided by the Super Block Company Limited, which had an average particle size of 34 μm. Al-containing waste (AW) was a residue from the secondary dross recovering process that was supplied by SRI Metal Products. AW was ground into three different finenesses. The finenesses of ground AW analysed by Laser particle size distribution (Malvern Mastersiser S Particle Size Analyser) were classified as high (AWS), medium (AWM) and low (AWL) with the mean particle sizes of 9.71, 29.91 and 51.11 μm, respectively, as shown in Fig. 6.1. The concentration of metallic aluminium present in AW was determined by measuring the amount of hydrogen gas production from the reaction between metallic aluminium powder and CaO (Fig. 6.2). The average metallic aluminium present in AW was 1.203±0.079% by weight. The chemical compositions of the materials used in this study were determined using X-ray fluorescence (XRF; WDXRF PW2400), which is shown in Table 3.2.

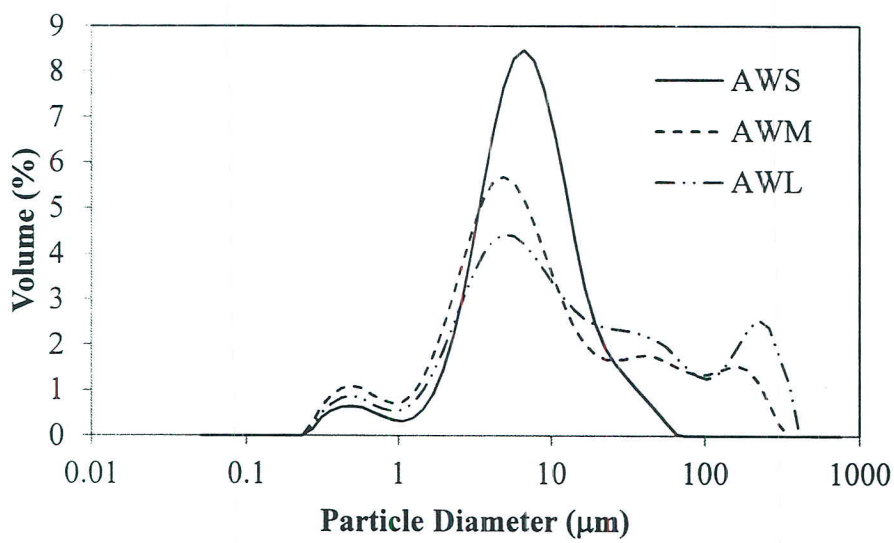

Figure 6.1 The particle size distribution of AW.

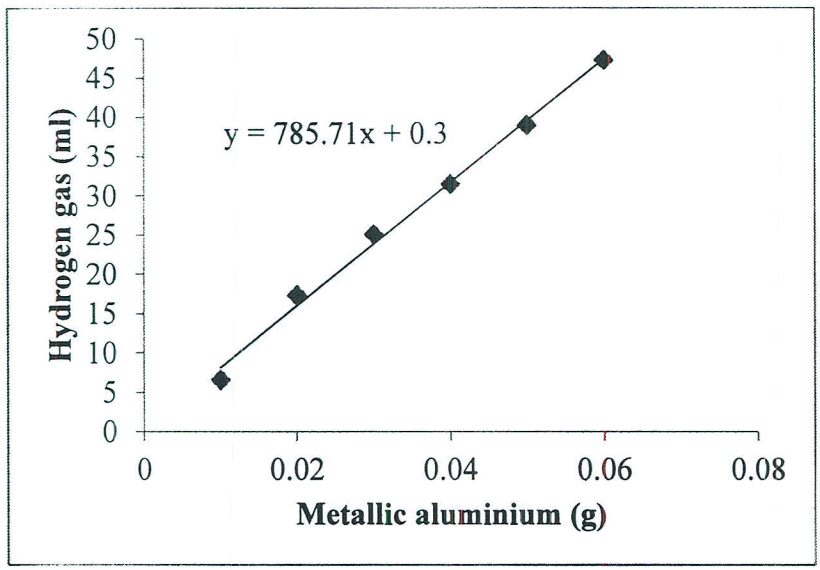

Figure 6.2 The relationship between the amount of metallic aluminium and the volume of hydrogen gas.

6.3 Experimental Procedure

In this study, the reference was prepared from ordinary Portland cement (OPC) 45, quick lime (CaO) 5, RHA 45, sand 5 and the addition of aluminium powder 0.5% by weight of binder (OPC+CaO). AW of various particle sizes was used to substitute for metallic aluminium at the level of 5%, 10%, 15% and 20% by weight. The overall mix proportions are summarized in Table 3.6. The solids were mixed in a Horbart mixer for 1min. Water was then added to give a water to binder (W/B) ratio of 1:1.25 and was continually mixed for 1 min and 30 sec. The slurry was poured into 5 cm cubic steel moulds. After casting, the samples were preheated in an oven at 40°C for 3 hr to achieve the desired setting and volume stability. The samples were then cured in an autoclave at 180°C for 4, 8 and 18 hr.

After autoclave curing, the samples used for the compressive strength test were dried at 40°C for 24 hr, to remove any excess moisture content of the sample to meet the requirements of ASTM C1368 [60]. The remaining samples were dried at 105°C for 24 hr then subjected to dry density measurement. For each mix proportion, a set of five samples was used for compressive strength and unit weight analysis. The average value of strength was reported to a variation of no more than 10%. After strength determination, the pieces

of cracked samples were used for microstructural analysis. The crystalline phases present in AAC samples were detected by XRD technique at a step size of 0.02°, a scan rate of 3° per min and scan range of 10° to 60° 2θ. The samples for scanning electron microscopy (SEM, JEOL-JSM-6400) analysis were dried by soaking in acetone and then coated with gold.

6.4 Results and Discussion

6.4.1 Dry Density

The oven-dry density variation of the specimens with high and low AW fineness, cured for 4 and 18 hr, are illustrated in Fig. 6.3. The results showed that AAC prepared from AW with high fineness has relatively lower dry density than those with low fineness at all mix proportions. It is generally known that a decrease in particle size causes an increase of surface area and corresponds to higher reactivity [24, 76]. As a result, samples containing AW with high fineness leads to an increase rate of reaction between metallic aluminium and calcium hydroxide ($Ca(OH)_2$) or alkali [18], as shown in Eq. 1.1, and generates more hydrogen gas bubbles which are present within the concrete specimen.

$$2Al + 3Ca(OH)_2 + 6H_2O \rightarrow 3CaO{\cdot}Al_2O_3{\cdot}6H_2O + 3H_2 \qquad (1.1)$$

It was also found that the increased level of AW substitution for aluminium powder caused a reduction in the dry density for all samples. This could be caused by the presence of aluminium oxide (Al_2O_3) in AW, which rapidly reacts with lime to produce calcium aluminate hydrate (CAH) during molding. The formation of CAH leads to the occurrence of flash setting in the AAC samples. This phenomenon could prevent the escape of hydrogen gas bubbles from the inside of the sample specimen and as a result, the dry density of the samples decreased with increasing AW content. In addition, a reduction of dry density from 2 to 6 % was observed from all samples compared to the reference.

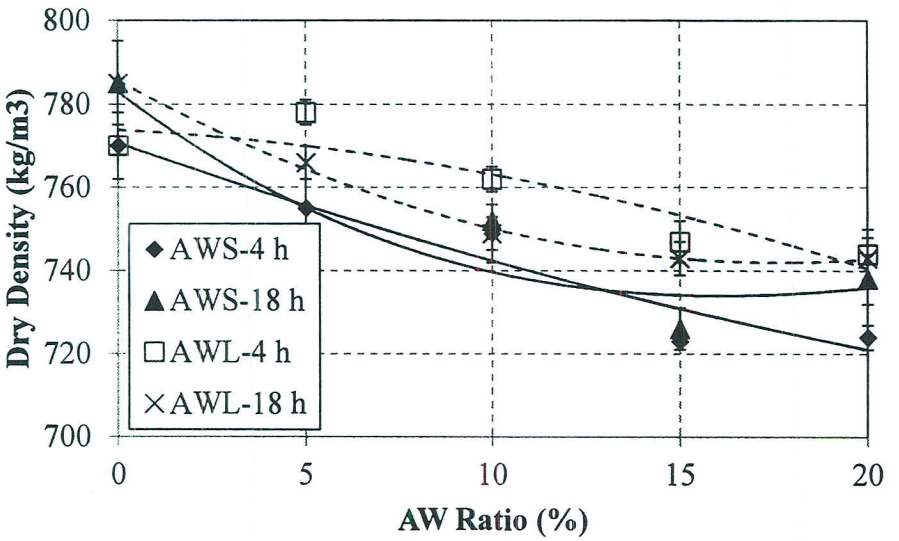

Figure 6.3 Dry density of AWC specimens.

6.4.2 Compressive Strength

Variations in compressive strength of all samples autoclaved for 4, 8 and 18 hr are illustrated in Fig. 6.4a-c. AAC samples with high fineness AW gave lower compressive strength than samples with medium and low finenesses AW for all autoclaving times. There are two reasons for this: the first is the rapid formation of CAH from the reaction between Al_2O_3 present in the high fineness AW with lime and covering the siliceous materials. This prevents the dissolution of silicate anions from the surface of siliceous materials and retards the formation of CSH which in turn affects the conversion of CSH to tobermorite due to insufficient silicate anions [58]. Another reason could come from the readily available Al_2O_3 present in the high fineness AW which is rapidly incorporated in the structure of CSH [59, 77]. The Al-substituted tobermorite is reported to be a poorly crystalline product which corresponds to a reduction in the strength of the AAC.

The strength of AAC decreased with increasing levels of AW replacement for metallic aluminium powder, except at the replacement level of 5% for medium and low finenesses of AW (Fig. 6.4a-c). This is because the Al species increased with the increase in AW content and accelerate the formation of Al-substituted tobermorite. In addition, at a high replacement level, the Al species can be absorbed on the surface of siliceous materials in all finenesses of AW observed resulting in a decreasing rate of dissolution of silicate anion species.

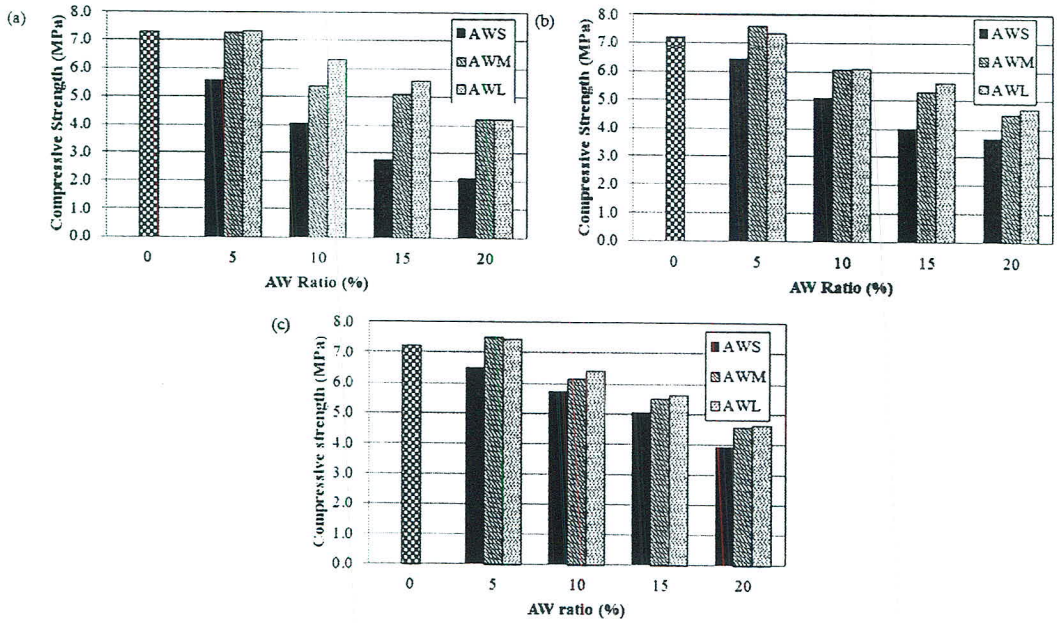

Figure 6.4 Compressive strength of AWC specimens. (a) 4 hr, (b) 8 hr and (c) 18 hr.

No significant effect of autoclaving time on the strength of AAC was observed except in samples containing high and medium finenesses of AW. At 4 hr autoclaving time, siliceous materials were covered with Al species, which retarded the dissolution of silicate anions [78-80] and resulted in fewer tobermorites both normal and Al-substituted being formed. When the autoclaving time was prolonged, the Al species that covered the siliceous materials were broken [80, 81]. Silicate anions were then released and reacted with normal CSH and transformed to either tobermorite or Al-substituted tobermorite, which improved the strength. From the experimental results, the AAC sample containing 10% low fineness AW and autoclave curing at a temperature of 180°C for 4 hr, meets ASTM C1386 standard class AAC-6 [60]. Several samples from this research work that meet both AAC class 4 and 6 are summarized in Table 6.1. The strength results found that it is not necessary to increase the fineness of AW to medium and high because this is energy and time consuming without any beneficial effect on strength development.

Table 6.1 The comparison between experimental results and physical requirements in accordance with ASTM C1386 [60].

Strength Class	Compressive Strength (min, MPa)	Density limits (kg/m^3)	Meet the Standard	
			4 hr	8 hr
AAC-4	4	650-750	10% AWS, and 20% AWM and AWL	15% AWS
AAC-6	6	750-850	10% AWL	5% AWS and 10% AWM

6.4.3 X-ray Diffraction Analysis (XRD)

The crystalline phases present in AAC samples containing 10 and 20% AW with low and high finenesses after autoclave curing for 4 and 18 hr are shown in Figs. 6.5 and 6.6. At 4 hr autoclaving time, only the peaks of quartz and tobermorite were observed for the reference sample (Fig. 6.5). Quartz appeared at 2θ of 21, 27, 40 and 50 degrees whereas tobermorite was found at 2θ of 29, 32 and 39 degrees. Similar XRD patterns were observed for the reference sample autoclave cured for 18 hr (Fig. 6.6). For AAC samples containing AW, the peaks of portlandite [$Ca(OH)_2$], at 2θ of 34 degrees, and katoite [K: $Ca_3Al_2(SiO_4)_{3-x}(OH)_{4x}$; x=1.5-3], at 2 ɵ of 34 degrees, appeared other than quartz and tobermorite for the sample containing 20% high fineness AW with an autoclaving time of 4 hr (Fig. 6.5). However, these two additional peaks of portlandite and katoite disappeared when the autoclaving time was extended to 18 hr.

At 4h autoclaving time, the rapidly-formed CAH interfered with the formation of CSH between silicate anions and $Ca(OH)_2$, which is why the peak of portlandite was observed. The presence of katoite which is a kind of hydrogarnet is reported to be formed through the conversion of metastable phases such as CAH and CASH [82]. However, at a longer autoclaving time (18 hr), katoite decomposed and transformed to tobermorite [58, 83]. This reaction indicates the other pathway for formation of tobermorite, in which has been reported by Matsui et al. (2011) [58], as given in Equation 6.1. They noted that katoite, a kind of hydrogarnet, is an important intermediate in tobermorite formation. Several studies also reported that, when kaolin and lime are used as starting materials, katoite was first reaction products and tobermorite was formed as further reaction time [84-

86]. Katoite was decomposed with increasing Si substitution into its own lattice and transformed to crystalline tobermorite. It facilitated inhibiting the conversion of tobermorite to xonotlite, extending the temperature range over which tobermorite exists. In addition, Mitsuda et al. (1992) [87] investigated the chemical composition of tobermorite crystals in AAC for various autoclaving times and reported that the Ca/(Al+Si) ratio also related with the formation of tobermorite. This is because that Al can be substituted into Si-tetrahedra of tobermorite and is called Al-substituted tobermorite [88]. For two pathways for formation of tobermorite, Matsui et al. (2011) [58] also concluded tobermorite was formed through pathway (I), as summarized in the previous chapter, at the early stage and pathway (II) became predominated in the late stage. This can be recommended that the initially formed CSH controls the two pathways of tobermorite.

Quartz, katoite, CSH $\rightarrow$ Si^{4+}, Ca^{2+}, Al^{3+}, OH^{-} $\rightarrow$ tobermorite (6.1)

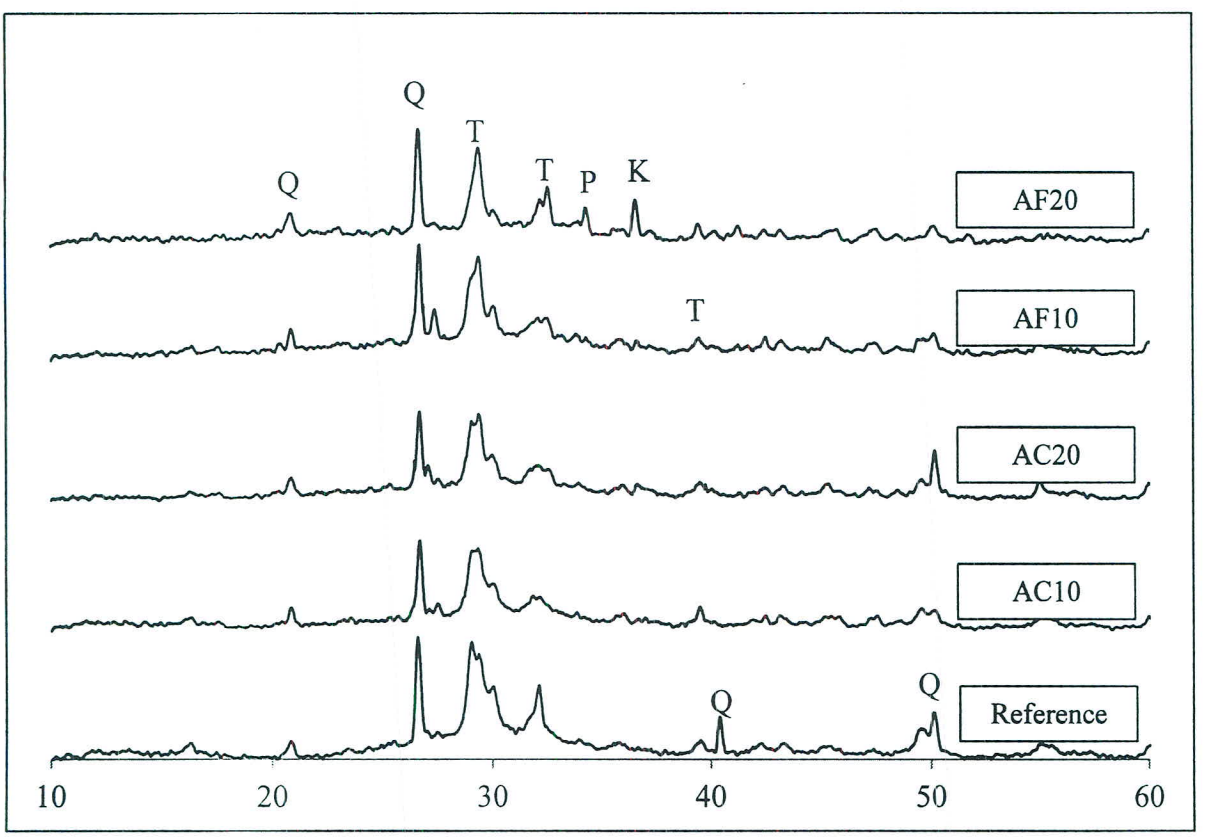

Figure 6.5 XRD patterns of AWC at 4 hr. T: tobermorite; P: portlandite; Q: quartz; K: katoite.

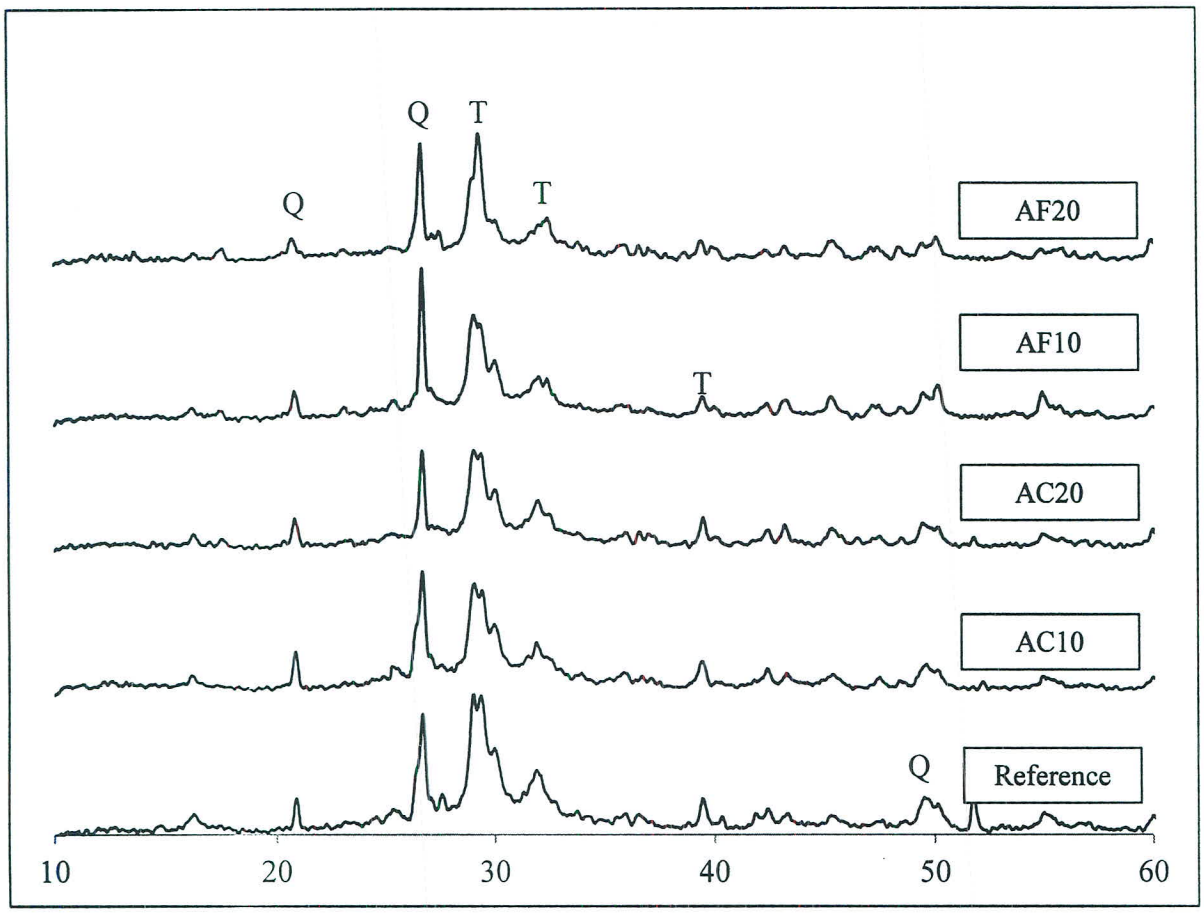

Figure 6.6 XRD patterns of AWC at 18 hr. T: tobermorite; Q: quartz.

6.4.4 Scanning Electron Microscopy (SEM)

SEM micrographs of AAC incorporating high and low finenesses of AW autoclaved at 180°C for 4 and 18 hr are shown in Fig. 6.7 and 6.9. At 4 hr of autoclave curing, the crumbled-foiled tobermorite was observed in the reference sample (Fig. 6.7a). When high fineness AW was introduced at 10%, the morphology of tobermorite was transformed to fibrous CSH and lath-like tobermorite (Fig. 6.7b). At increasing amounts of high fineness AW to 20% (Fig. 7c), fibrous CSH instead of tobermorite was observed throughout the SEM image. In AAC samples containing 10% and 20% low fineness AW, both lath-like and plate-like tobermorites were found (Fig. 6.7d and 6.7e).

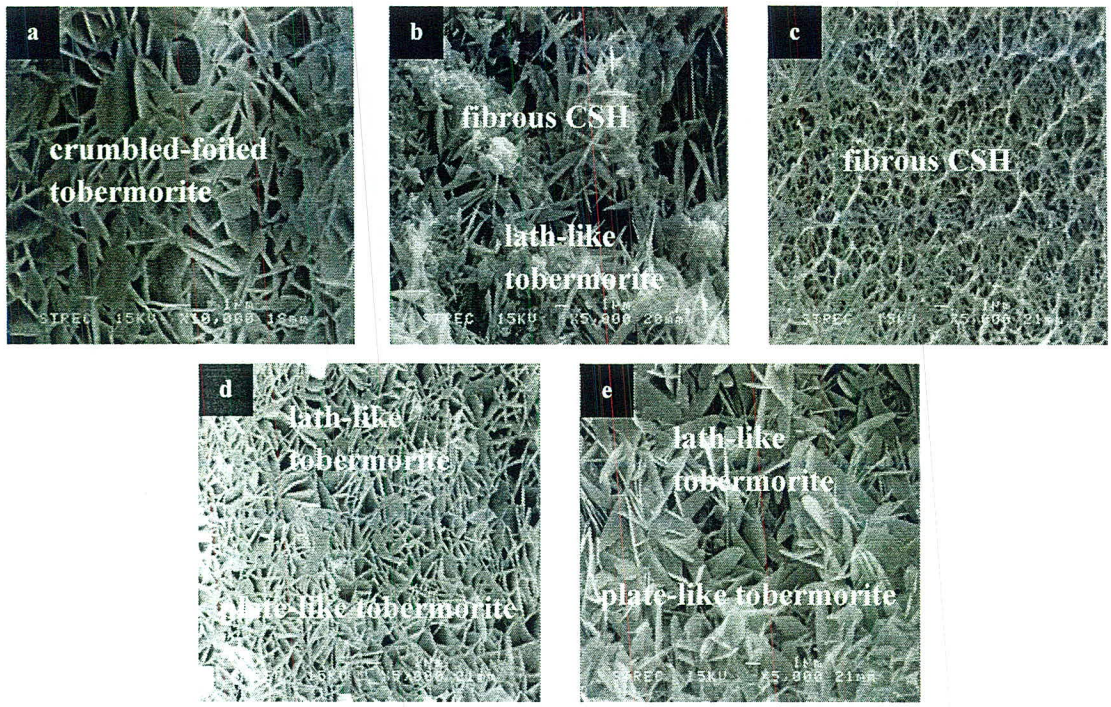

Figure 6.7 SEM micrographs of AWC specimens at 4 hr: (a) reference, (b) AWS-10, (c) AWS-20, (d) AWL-10 and (e) AWL-20.

For normal cement hydration, C_3S and C_2S started to hydrate at the beginning of the hydration process and the hydration products, Ca-rich CSH and $Ca(OH)_2$, were obtained. Under autoclave curing at increasing temperature and pressure, the dissolution of silicate anions from siliceous materials (quartz sand and RHA) increases and rapidly reacts either with Ca-rich CSH or $Ca(OH)_2$ to form crystalline tobermorite. Taylor [21] reported that tobermorite can be readily synthesized under hydrothermal treatment using $Ca(OH)_2$ and finely ground quartz at a temperature of 180°C. This agrees with the XRD results when the peak of $Ca(OH)_2$ was not found except at 20% high fineness AW. In the presence of 20% high fineness AW, the ettringite, CAH and aluminium hydroxide ($Al(OH)_3$) were obtained during the first 30 min of moulding (Fig. 6.8a) and changed to CASH with prolonged moulding for 3 h (Fig. 6.8b). This finding agreed with the above mentioned on the dissolution retardation of silicate anions by the covering of CAH on the siliceous materials. Also, the increased amount of Al_2O_3 enhanced the formation of CASH during moulding and transformed to lath-like tobermorites, which is a form of Al-substituted tobermorite [88, 89]. Moreover, this dissolution retardation of silicate anions by AW

causes the Ca/Si ratio of the system to increase to the level that is favourable for the formation of plate-like tobermorites [2].

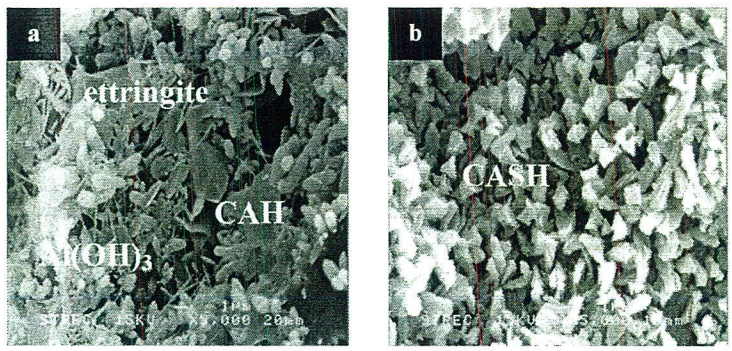

Figure 6.8 The morphology of AAC containing 20% high fineness AW during moulding. (a) at 30 min and (b) at 3 h.

With an increase in autoclaving time to 18 h, the crumbled-foiled tobermorite was still observed from the reference sample (Fig. 6.9a), whereas lath-like and plate-like tobermorites were found in AAC samples containing both high and low finenesses AW (Fig. 6.9b-e). The presence of crumbled-foiled tobermorite in the reference AAC samples of both autoclaving times (4 and 18 h) shows good agreement with XRD and compressive strength results. This indicates that 4 h autoclave curing is enough for an AAC sample without AW. In the presence of high fineness AW, an increased autoclave curing from 4 to 18 h can transform fibrous CSH to lath-like and plate-like tobermorites, which enhances strength by 37% and 97% for samples containing 10% and 20% AW, respectively.

6.5 Conclusions

This study aims at the use of two types of waste residues, RHA and AW, as raw materials in AAC. The effect of AW finenesses on the physical, mechanical and microstructural properties of AAC are as follow:

- The replacement of metallic Al by AW in AAC decreased the strength and dry density of the products, except at the replacement level of 5% of medium and low finenesses AW after 8 hr autoclave curing.

- The presence of high fineness AW interfered the dissolution of silicate anion from RHA and quartz sand, and as a result, the formation of tobermorite was retarded at 4 hr autoclave curing. However, under prolong autoclave curing, the Al species that were adsorbed on the siliceous materials were decomposed and either normal or Al-substituted tobermorite were formed.
- SEM images revealed that AW affects the morphology of the reference sample through the transformation of the crumbled-foiled tobermorite to plate-like which is normal tobermorite and lath-like tobermorite, which is Al-substituted tobermorite.
- RHA and AW are successfully used as raw materials in AAC to replace fine aggregates and expansive agents (metallic Al), and to produce AAC that meets the ASTM standard class 6 on sample containing 10% low fineness AW and autoclave curing at 180°C for 4 hr.

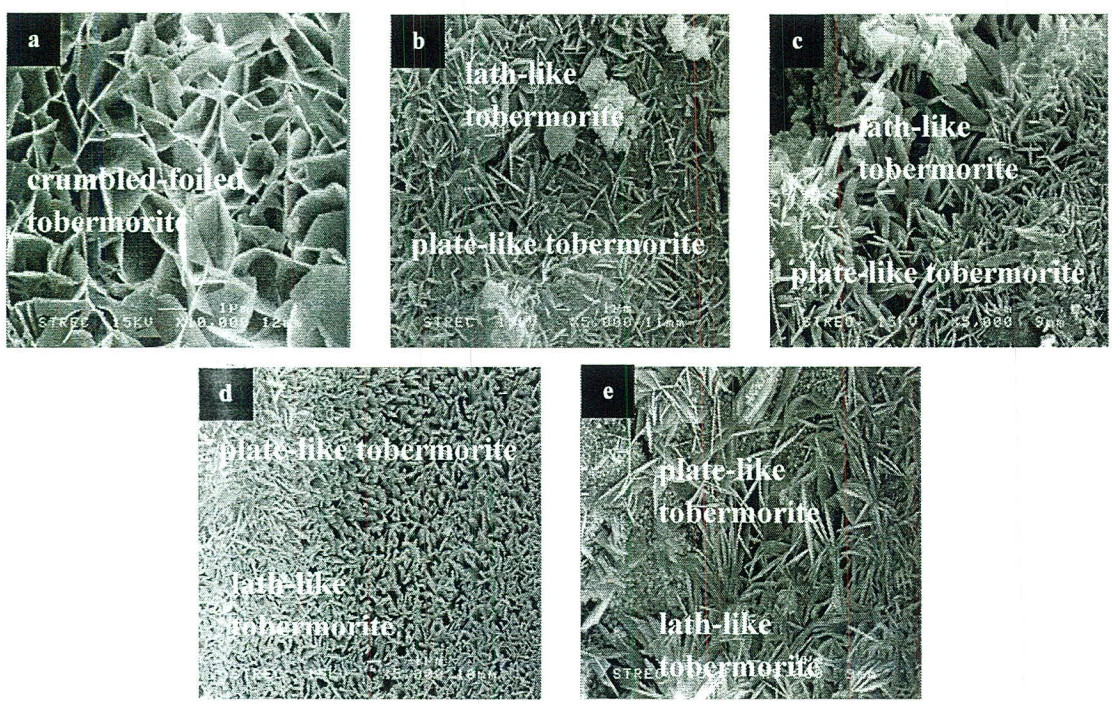

Figure 6.9 SEM micrographs of AWC specimens at 18 hr: (a) reference, (b) AWS-10, (c) AWS-20, (d) AWL-10 and (e) AWL-20.